Investigation of the Effect of Harmonics Caused by Transformer-Induced Nonlinear Loads on Electrical Energy

Sabir Rüstemli[1], Nejdet Sezgin[1,2], Bilal Coşkun[3] and Gökhan Şahin[4],*

[1] Electrical and Electronics Engineering Department, Bitlis Eren University, Bitlis, 13000, Türkiye

[2] Vocational School of Technical Sciences, Department of Electricity and Energy, Mus Alparslan University, MuŞ, 49001, Türkiye

[3] Vocational School of Technical Sciences, Electronics and Automation, Mus Alparslan University, MuŞ, 49001, Türkiye

[4] Copernicus Institute of Sustainable Development, Utrecht University, Utrecht, 3584 CB, The Netherlands

INFORMATION

Keywords:
Harmonics
energy quality
active parallel power filter
Matlab/Simulink

DOI: 10.23967/j.rimni.2025.10.64634

SCIPEDIA
Revista Internacional de Métodos Numéricos para Cálculo y Diseño en Ingeniería

Investigation of the Effect of Harmonics Caused by Transformer-Induced Nonlinear Loads on Electrical Energy

Sabir Rüstemli[1], **Nejdet Sezgin**[1,2], **Bilal Coşkun**[3] **and Gökhan Şahin**[4,*]

[1]Electrical and Electronics Engineering Department, Bitlis Eren University, Bitlis, 13000, Türkiye

[2]Vocational School of Technical Sciences, Department of Electricity and Energy, Mus Alparslan University, Muş, 49001, Türkiye

[3]Vocational School of Technical Sciences, Electronics and Automation, Mus Alparslan University, Muş, 49001, Türkiye

[4]Copernicus Institute of Sustainable Development, Utrecht University, Utrecht, 3584 CB, The Netherlands

ABSTRACT

In this study, distribution transformers in the Muş Alparslan University campus are analyzed in order to minimize energy losses due to harmonics in the electrical network. Current and voltage harmonics, which are the power quality problems of these transformers, are analyzed. The power quality of different transformers in Muş Alparslan University was measured with a Chauvin Arnoux CA:8331 energy analyzer. Three-phase nonlinear load models were created using current harmonic values in the Matlab/Simulink environment. A parallel active power filter is designed in the Matlab/Simulink environment to eliminate current harmonics. The performance of the parallel active power filter is analyzed for each transformer. As a result, the total harmonic distortion (THDI) ratio for the current decreased from 6.78% to 1.38% in fast Fourier transform analyses after the parallel active power filter was activated in the first transformer. Similarly, the THDI ratio decreased from 5.1% to 2.19% in the second transformer, from 4.5% to 1.39% in the third transformer, and from 5.63% to 1.36% in the fourth transformer.

OPEN ACCESS

Received: 20/02/2025

Accepted: 15/04/2025

Published: 30/05/2025

DOI
10.23967/j.rimni.2025.10.64634

Keywords:
Harmonics
energy quality
active parallel power filter
Matlab/Simulink

1 Introduction

The energy transmission system serves as the core structure of an electrical power network. The quality of electrical energy within this system is primarily determined by the continuity of the electricity supply, voltage and frequency variations remaining within acceptable limits, and the smoothness of the waveform. For electric power systems to function reliably, various factors must be accounted for during both the design and operation stages. One of these critical factors is the presence of harmonics generated by nonlinear components, which significantly influence power quality. Nonlinear elements in electrical systems lead to harmful harmonic distortion in transmission and distribution networks, compromising the overall quality of the electricity delivered to consumers [1,2]. The issue of harmonics was first identified in 1893 when engineers were investigating engine heating problems in Hartford and discovered that the primary source of heat was resonance in the connected power

*Correspondence: Gökhan Şahin (g.sahin@uu.nl).

system. They determined that this resonance stemmed from the variable waveforms, or harmonics, present in the system [3]. Even earlier, in 1890, electricians in Portland were addressing problems with transmission lines potentially caused by line frequency harmonics. These early investigations mark the first documented analyses of harmonics in power systems. At that time, European electricity producers were largely unaffected by such problems, as they were not utilizing high frequencies in their systems [3]. However, as technology advanced, harmonic distortion became a global concern, prompting the development of various techniques to detect and mitigate these harmful waves. In one notable study on industrial furnaces controlled by a 12-pulse converter in Alabama, researchers conducted harmonic analysis on both current and voltage. Using simulations, they identified that harmonics such as the 5th, 7th, 11th, and 13th were being injected into the furnace system by the converter [4]. This analysis was conducted in compliance with the IEEE-519 standard, which recommended the use of tuned shunt or parallel Inductor-Capacitor (LC) filters for each phase to mitigate these harmonics. Similarly, other studies have explored harmonic analysis in variable load motor circuits, revealing the presence of harmonic currents and voltages [5,6]. Even in systems with smaller power ratings, harmonic behavior has been analyzed, such as in circuits with nonlinear loads controlled by single-phase full-wave rectifiers [7]. The generation of harmonics is a persistent and unavoidable issue, with nonlinear loads being a significant contributor to harmonic disturbances in electrical systems. As the use of nonlinear elements increases across industries, the importance of addressing harmonic pollution grows, and it poses a significant threat to the reliability of electrical power systems. Consequently, accurately measuring and analyzing harmonic sources has become a crucial task for the efficient control and analysis of power systems [8,9]. Harmonic analysis plays a pivotal role in ensuring optimal power quality in electrical systems [10]. Given the complexity of electrical networks, these analyses are often performed using simulation environments. Previous research has investigated how transformer connection groups affect harmonics [11–14]. However, there remains a lack of studies using electrical models derived from real-world data obtained from large distribution networks. This research aims to bridge that gap by simulating a large distribution network and examining how changes in transformer connection groups influence harmonics within the system. For instance, time-dependent voltage and current vectors are analyzed through various transformation techniques, such as the DQ Transform [15–18], PQ Transform [19–21], and machine learning models like back propagation [22–24] and adaptive extraction methods [25–27]. These techniques decompose the signals into their components, and control algorithms such as Proportional-Integral (PI) or Proportional-Integral-Derivative (PID) controllers are employed to generate compensation signals. In addition, studies have analysed specific applications, such as the energy quality of an educational building [28–31], and obtained findings showing that load distribution imbalances lead to reactive power problems in compensation systems. Balancing the loads and applying passive filters helped achieve the desired power quality standards. Similar studies at university campuses have investigated harmonic levels in transformer panels, using passive filters to reduce high harmonic ratios [32–36]. Further research has explored the effects of intermediate harmonics generated by nonlinear loads on power quality, demonstrating how series active filters can reduce harmonic distortion by significant percentages in different load systems [37–39]. Overall, with the increasing reliance on power electronics and nonlinear devices, harmonics in the power system have become a critical issue. Harmonics not only result in additional losses but also pose risks such as faulty tripping in protection systems, overheating of electrical machines and power lines, and efficiency losses. These adverse effects make the detection and mitigation of harmonics an important area of research. Furthermore, power quality limits in distribution networks are governed by standards such as EN50160, outlined in regulations by the Energy Market Regulatory Authority (EMRA) [40–43]. In another study, the Gazelle Optimisation Algorithm (GOA) improved with a chaotic maps algorithm is proposed for the estimation of harmonics and sub/inter harmonics to solve power quality problems caused by harmonics. Ten chaos-based GOA variants were analyzed for noisy and noiseless conditions using 2 synthetic power signals and a time-varying signal. In the performance analysis, the Gauss/Mouse chaotic map-based GOA (G/M GOA) method outperformed the other methods and estimated the amplitude, frequency, and phase parameters with high accuracy [44]. In another study, it was reported that conventional FFT analysis is sensitive to noise and has low-frequency resolution when detecting harmonics and inter-harmonics. The PEA (parameter estimation algorithm) method is proposed to overcome this problem. It is reported that this proposed method is more robust to noise and estimates the frequency, phase, and amplitude parameters of harmonics and interharmonics with high accuracy in a shorter time and provides twice the accuracy compared to the windowed FFT and Prony algorithm [45].

This study analyzes the energy quality of Muş Alparslan University Campus with a focus on harmonics. Data, including total harmonic distortion (THD), voltage fluctuations, and phase current imbalance, were collected from low-voltage transformer measurements across the campus. The analysis revealed that while the voltage harmonics complied with the relevant standards, there were significant current harmonics present. To address this issue, a simulation of the current harmonics was carried out in a computer environment. Subsequently, a parallel active power filter was designed and implemented, resulting in a substantial reduction of the current harmonics.

1.1 Study Area

Muş Alparslan University, established in 2007, currently operates with 10 faculties, 6 vocational schools, and 2 institutes as of 2024. The university campus is situated in the Güzeltepe neighborhood, covering an area of 130,000 m^2 with a total enclosed space of 193,865 m^2. The campus receives its energy supply via a 477 MCM 34.5 kV power transmission line from the city center. Upon entering the Güzeltepe modular cell, the 477 MCM line is connected to the first transformer on the campus through a 95 mm^2 XLPE cable. The campus is equipped with five transformer modular cells, with connections between transformers facilitated by XLPE cables running through the gallery. Fig. 1 illustrates the medium voltage energy distribution system and the transformer capacities across the campus.

2 Materials and Methods

This section outlines the methods and equipment used for harmonic measurements at Muş Alparslan University Campus. Initially, the instruments employed to measure current and voltage harmonics will be introduced, along with the data collected from these devices. Following this, the process of transferring the gathered data into the simulation environment will be explained. Finally, a parallel active power filter will be designed in the Matlab/Simulink environment to reduce the harmonic levels based on the obtained data.

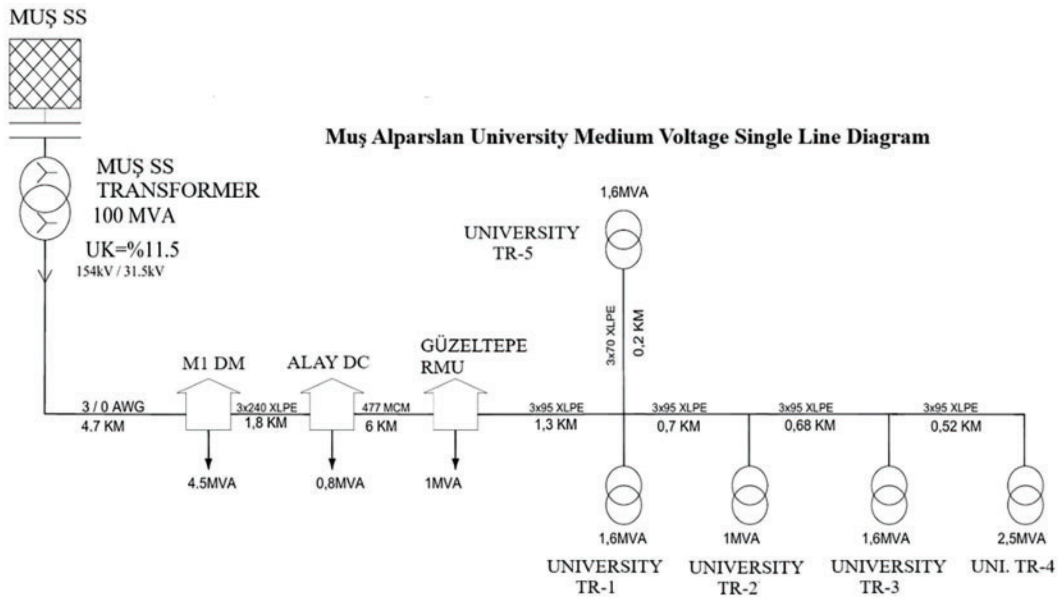

Figure 1: Muş Alparslan university medium voltage power distribution infrastructure and transformer power single line diagram

2.1 Mathematical Calculations of Harmonics

In a power system, current and voltage waveforms are ideally desired to be sine waves. However, in practical applications, the waveform of current and voltage due to non-linear loads in the power system is not an ideal sine wave. These non-ideal composite waves in current and voltage are defined as harmonics. Harmonics are expressed mathematically with the help of the Fourier series. In Fourier transform, non-sinusoidal signals are written as the sum of signals of different amplitude and frequency [46,47]. Fourier series expansion of a periodic wave is given in Eqs. (1) and (2).

$$f(t) = \frac{a_0}{2} + \sum_{n=1}^{\infty} a_n \cos(n\omega t) + \sum_{n=1}^{\infty} b_n sin(n\omega t) \tag{1}$$

$$f(t) = \frac{a_0}{2} + a_1 \cos(\omega t) + b_1 \sin(\omega t) + a_2 \cos(2\omega t) + b_2 \sin(2\omega t) + \cdots) \tag{2}$$

in these equations a_0, a_n, b_n are the coefficients and the angular velocity ω is $2\pi/\mathrm{T}$. The coefficients are calculated as in Eqs. (3)–(5).

$$a_0 = \frac{1}{T}\int_0^T f(t)dt \tag{3}$$

$$a_n = \frac{2}{T}\int_0^T f(t)\cos(n\omega t)dt \tag{4}$$

$$b_n = \frac{2}{T}\int_0^T f(t)\sin(n\omega t)dt \tag{5}$$

2.1.1 Filtering Harmonics

Harmonic sources, i.e., harmonic-generating devices (transformers, rectifiers, arc furnaces, lighting elements, etc.), should be designed to produce little or no harmonics when manufactured. However, this may not be possible in practical applications. The equipment added to the power system in order to minimise current and voltage harmonics and to design the network to be affected by harmonics is called a 'harmonic filter'. These circuits are used to filter or suppress the desired harmonics. Harmonic filters are used to reduce or eliminate the level of voltage or current harmonics at one or more frequencies [47–49]. Two different methods are used to minimise harmonics in power systems. These methods are known as the filtering method or the harmonic suppression method after the harmonic occurs. Harmonic filters are 'Passive filters' consisting of circuit elements such as resistance, inductance, and capacitance, and 'Active filters' with controlled voltage or current source [50].

2.1.2 Total Harmonic Distortion (THD)

THD can be defined as the percentage deviation of the harmonic component from the ideal waveform. At the fundamental frequency, the total harmonic distortion is zero. Total harmonic distortion is the square root mean of the harmonic components of a waveform divided by the fundamental component. The total harmonic distortion voltage is calculated as in Eq. (6) below. In Eq. (6), THD_V is expressed as total harmonic distortion concerning voltage. V_n is the nth order voltage harmonic V_1 is the voltage at fundamental frequency.

$$THD_V = \frac{\sqrt{\sum_{n=2}^{\infty} V_n^2}}{V_1} \tag{6}$$

total harmonic distortion current is calculated by Eq. (7). Here, THD_I is defined as the total harmonic distortion in the current, I_n is the nth order current harmonic, I_1 is the current at fundamental frequency.

$$THD_I = \frac{\sqrt{\sum_{n=2}^{\infty} I_n^2}}{I_1} \tag{7}$$

2.1.3 Total Demand Distortion (TDD)

Total demand distortion (TDD) is the average of the maximum currents demanded by the load. *TDD* is a load-related variable and can be calculated according to Eq. (8).

$$TDD = \frac{\sqrt{\sum_{n=2}^{\infty} I_n^2}}{I_L} \tag{8}$$

2.1.4 Shape Factor

The shape factor is a parameter that expresses a certain characteristic of the waveform of a signal. In power systems, the shape factor is usually defined as the ratio of the effective value of a current or voltage signal to its average value. It is calculated as in Eq. (9).

$$k_{f=}\frac{Ef\ ektif\ Değer}{Ortalama\ Değer} \tag{9}$$

2.1.5 Peak Factor

Peak factor is the ratio between the peak value of the harmonic signal and the effective value of the fundamental component [51,52]. More precisely, for a current or voltage that is not in the form of an ideal sine wave, the peak factor value is calculated by dividing the peak value by the effective value of the fundamental component as in Eq. (10).

$$Peak\ Factor = \frac{Peak\ Value}{Effective\ Value\ of\ the\ Basic\ Component} \tag{10}$$

2.1.6 Distortion Power Factor

One-phase nonlinear loads that generate high current distortion require power factor calculation. Since these loads cause resonance, power factor calculation and power factor corrector elements should be used [53]. The following Eq. (11) is used for voltage:

$$V = V_1\sqrt{1 + \left(\frac{THD_V}{100}\right)^2} \tag{11}$$

the following Eq. (12) is used for current:

$$I = I_1\sqrt{1 + \left(\frac{THD_I}{100}\right)^2} \tag{12}$$

active and passive filters are used to maximise the distortion power factor and to eliminate harmonics produced by nonlinear loads [54].

2.1.7 Harmonic Standards

EN 50006 and IEEE-519-1992 define standards for current and voltage harmonics to improve electrical power quality. Total harmonic distortion (THD) refers to the distortion in voltage and current waves. THD is calculated as the ratio of the sum of the effective values of the harmonics to the effective value of the fundamental component. According to IEEE 519, this ratio is defined as 5.0% for current harmonics and 3.0% for voltage harmonics in power systems below 69 kV. IEEE Std 519-1992 standard considers concepts such as THD and TDD when determining harmonic distortion limits. While THD indicates the harmonic levels according to the instantaneous load condition, TDD takes into account the long-term load condition of the system. Therefore, TDD prevents the misinterpretation of harmonic levels in light load cases [55].

2.2 Purpose of Measurements in Energy Quality in Electrical Systems

Instantaneous power theory is one of the methods used in active power filter control. This theory was proposed by Akagi in 1983. Instantaneous power theory (IPT) is known as a simple calculation method that gives output with instantaneous values in three-phase systems. In this method, the instantaneous active and reactive powers of the three-phase system can be calculated instantaneously regardless of whether the system is harmonised and/or unbalanced. In this method, also known as p and q theory, firstly, three-phase components (abc) are converted into two-phase components ($\alpha\beta$) by means of Clarke transformation. Using the transformed currents and voltages, the instantaneous values of active and reactive powers are calculated with the help of instantaneous power theory. The instantaneously calculated powers consist of Alternating Current (AC) and Direct Current (DC) components [56,57]. Clarke's transformation of currents and voltages are given in Eqs. (13) and (14).

$$\begin{bmatrix} i_0 \\ i_\alpha \\ i_\beta \end{bmatrix} = \sqrt{\frac{2}{3}} \begin{bmatrix} 1/\sqrt{2} & 1/\sqrt{2} & 1/\sqrt{2} \\ 1 & -1/2 & -1/2 \\ 0 & \sqrt{3}/2 & -\sqrt{3}/2 \end{bmatrix} \begin{bmatrix} i_a \\ i_b \\ i_c \end{bmatrix} \tag{13}$$

$$\begin{bmatrix} V_0 \\ V_\alpha \\ V_\beta \end{bmatrix} = \sqrt{\frac{2}{3}} \begin{bmatrix} 1/\sqrt{2} & 1/\sqrt{2} & 1/\sqrt{2} \\ 1 & -1/2 & -1/2 \\ 0 & \sqrt{3}/2 & -\sqrt{3}/2 \end{bmatrix} \begin{bmatrix} V_a \\ V_b \\ V_c \end{bmatrix} \tag{14}$$

the instantaneous active and reactive power matrix is calculated as in Eq. (15). Where p and q are active and reactive (virtual) power, respectively. Normally, only the average value of the instantaneous real power is desired in the power system. Other power components are eliminated by using an active power filter. In addition to the instantaneous power components, the active power filter also has a power requirement to stabilise the capacitor voltage on the DC bus side [56,57].

$$\begin{bmatrix} p \\ q \end{bmatrix} = \begin{bmatrix} V_\alpha & V_\beta \\ -V_\beta & V_\alpha \end{bmatrix} \begin{bmatrix} i_\alpha \\ i_\beta \end{bmatrix} \tag{15}$$

biaxial currents can be obtained from the obtained powers as in Eq. (16).

$$\begin{bmatrix} i_\alpha \\ i_\beta \end{bmatrix} = \frac{1}{{V_\alpha}^2 + {V_\beta}^2} \begin{bmatrix} V_\alpha & V_\beta \\ V_\beta & -V_\alpha \end{bmatrix} \begin{bmatrix} \tilde{p} & -\bar{p} \\ q & \end{bmatrix} \tag{16}$$

by converting the reference currents obtained on the two axes to the three-phase system by means of the inverse Clarke transformation, the reference currents for the three-phase system can be obtained as in Eq. (17).

$$\begin{bmatrix} i_{a\_ref} \\ i_{b\_ref} \\ i_{c\_ref} \end{bmatrix} = \sqrt{\frac{2}{3}} \begin{bmatrix} 1/\sqrt{2} & 1 & 0 \\ 1/\sqrt{2} & -1/2 & -\sqrt{3}/2 \\ 1/\sqrt{2} & -1/2 & -\sqrt{3}/2 \end{bmatrix} \begin{bmatrix} i_0 \\ i_\alpha \\ i_\beta \end{bmatrix} \tag{17}$$

2.3 Measuring Harmonics

In order for the electricity quality in electrical power systems to be at the specified standards, it should be monitored regularly, measurements should be taken, and analyses should be made. With the data obtained, solution methods for the problems that occur or may occur should be investigated. Power quality problems can be detected by fixed devices or portable devices connected to the facility. Especially in industrial plants with continuous operation and high energy consumption, there should be power quality analyzers that continuously monitor the system. It is an important advantage that the information obtained can be stored electronically. Since such devices record continuously, they provide the opportunity to see and analyze the energy quality of the facility and to intervene quickly. Transformer modular cells low voltage (LV) panel harmonic measurements are shown in Fig. 2.

In electrical systems, the efficient operation of power systems and electrically powered devices relies on the transmission, distribution, and consumption of ideal voltage and current, typically represented by a 50 Hz sine wave. However, disturbances from equipment within the system or from consumers connected to the grid can cause the fundamental electrical quantities—such as flux, current, and voltage—to deviate from this ideal sinusoidal waveform. These disturbances, such as unwanted harmonic currents and voltages, which are integer multiples of the fundamental frequency, can significantly distort the original waveform. Issues like sudden voltage fluctuations, instantaneous interruptions, voltage extremes, harmonic distortions, waveform anomalies, and frequency shifts can all be monitored and addressed through power quality analyzers. In this study, the Chauvin Arnoux 8331 power analyzer (Chauvin Arnoux Ltd., Dewsbury, UK) was utilized to measure the harmonic levels in the transformer LV panels. This device is capable of generating power quality reports in line with EN50160 standards and is designed for quick and efficient analysis of large datasets. Featuring a large color graphic screen, the CA: 8331 ensures ease of use and accessibility. The analyzer can measure current and voltage harmonics up to the 50th harmonic, record voltage waveforms, and log data on active, reactive, and apparent power, as well as active and reactive energy. Additionally, it records flicker and provides the ability to transfer all recorded data to a computer. The device is also suitable for conducting comprehensive energy audits of a building's electrical system. A picture of the CA: 8331 energy analyzer used for measurements at Muş Alparslan University Campus is shown in Fig. 3.

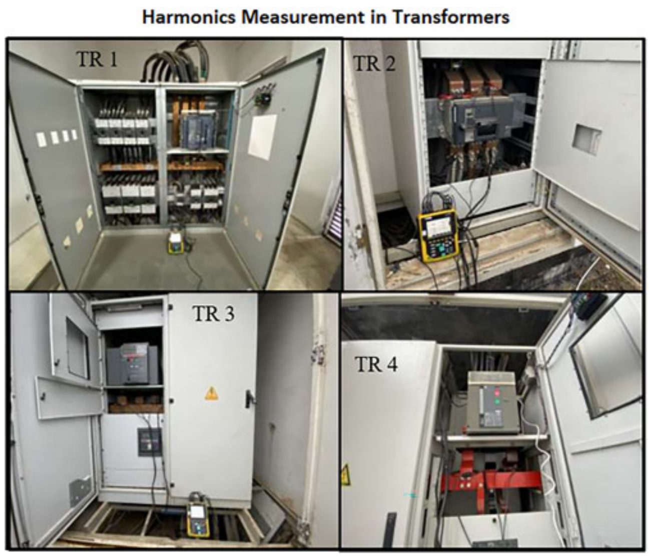

Figure 2: Transformer modular cells low voltage panel harmonic measurements

Figure 3: Chauvin Arnoux CA: 8331 energy analyzer

2.4 Parallel Active Power Filter Design

Although parallel active power filters are effective in reducing harmonics, some difficulties arise in practice. Unlike the simulation environment, in real-time applications, load and grid conditions are not constant but vary. This situation requires that the control algorithm to be used should react quickly according to the variable grid and load conditions; in other words, adaptive control methods are needed. In addition, switching losses and electromagnetic interference (EMI) are critical for system stability in real-time applications. From a cost point of view, the price differences between high-performance digital signal processing (DSP) and power electronics equipment and passive filters required for real-time active power filter (AGF) applications have become more reasonable today [58]. In this study, the harmonic data measured in real time are transferred to the Matlab/Simulink environment, and the liberty variance format (LVF) to suppress the harmonics measured in the Matlab/Simulink environment is designed. The single-line schematic of the parallel active power filter is given in Fig. 4.

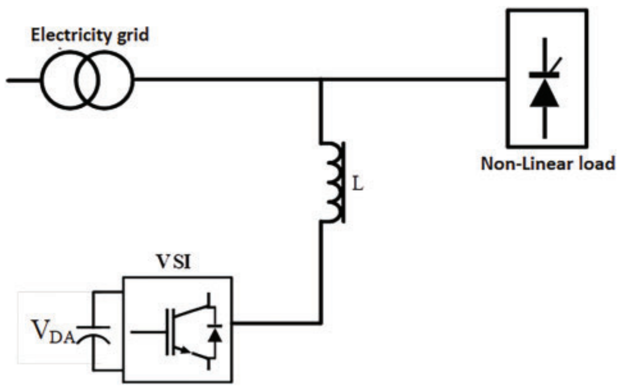

Figure 4: Single line schematic of parallel active power filter

In this study, a Matlab/Simulink model on the elimination of harmonics using the instantaneous power (*p* and *q*) theory is created. Instantaneous powers (*p* and *q*) are calculated using three phase currents and voltages. The power at fundamental frequency (50 Hz) was obtained by applying *p*, which constitutes the instantaneous active power and includes all harmonics, to a low-pass filter. This fundamental frequency power was subtracted from the power containing all harmonics, and the harmonic power to be filtered was separated. Finally, using these powers and three-phase voltages, reference currents are obtained at the output of the parallel active power filter to eliminate the grid harmonics. Since reactive power compensation is not performed in this study, instantaneous reactive power q is not included in the calculation. Fig. 5 shows the transformation of three-phase currents into biaxial currents by Clark transformation.

Fig. 6 shows the transformation of three-phase voltages into biaxial voltages by means of Clark transformation.

After Clark's transformations of three-phase currents and voltages, *p* and *q* powers were obtained by instantaneous power theory using the biaxial currents and voltages obtained as shown in Fig. 7.

After the *p* and *q* powers were calculated, three-phase reference currents were obtained using these powers. Fig. 8 shows the reference current calculation model of the parallel active power filter.

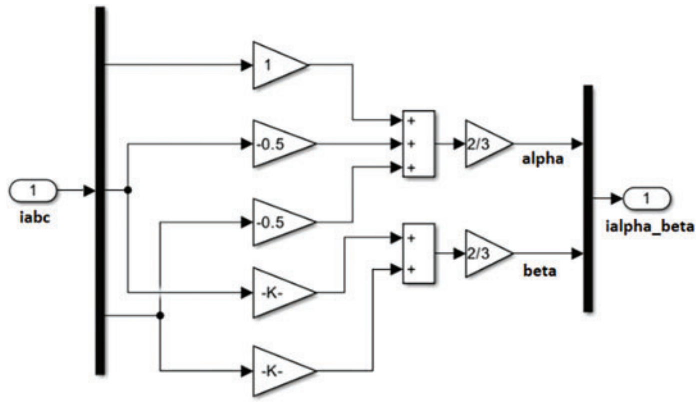

Figure 5: Clark transformation of three-phase currents

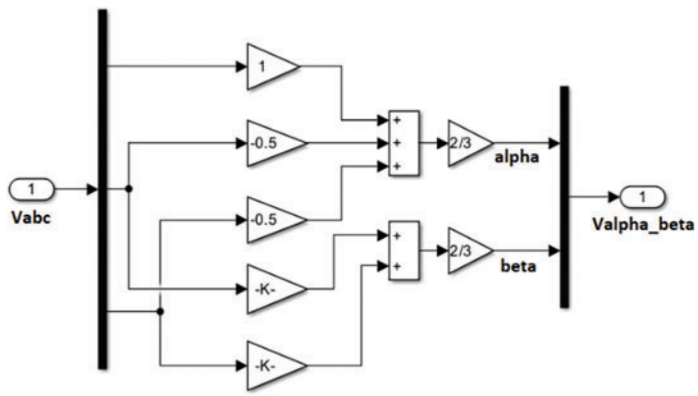

Figure 6: Clark's transformation of three-phase voltages

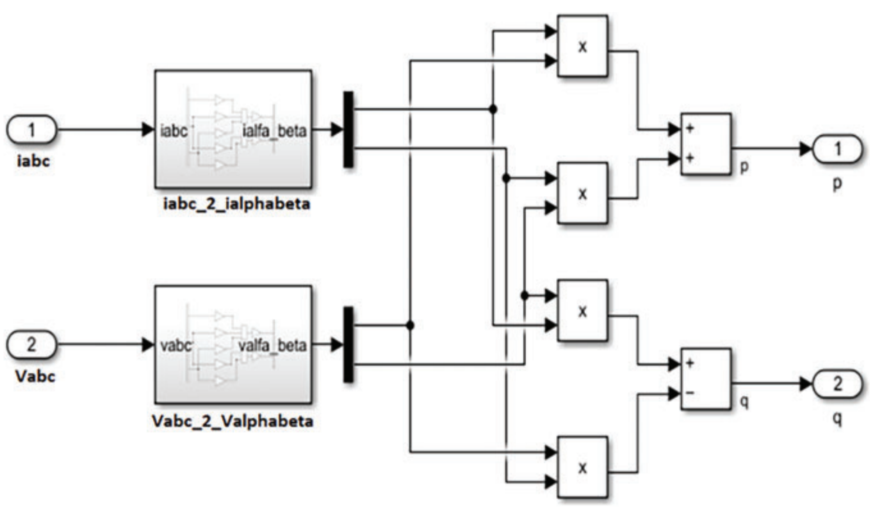

Figure 7: Matlab/Simulink model of instantaneous p and q power calculation

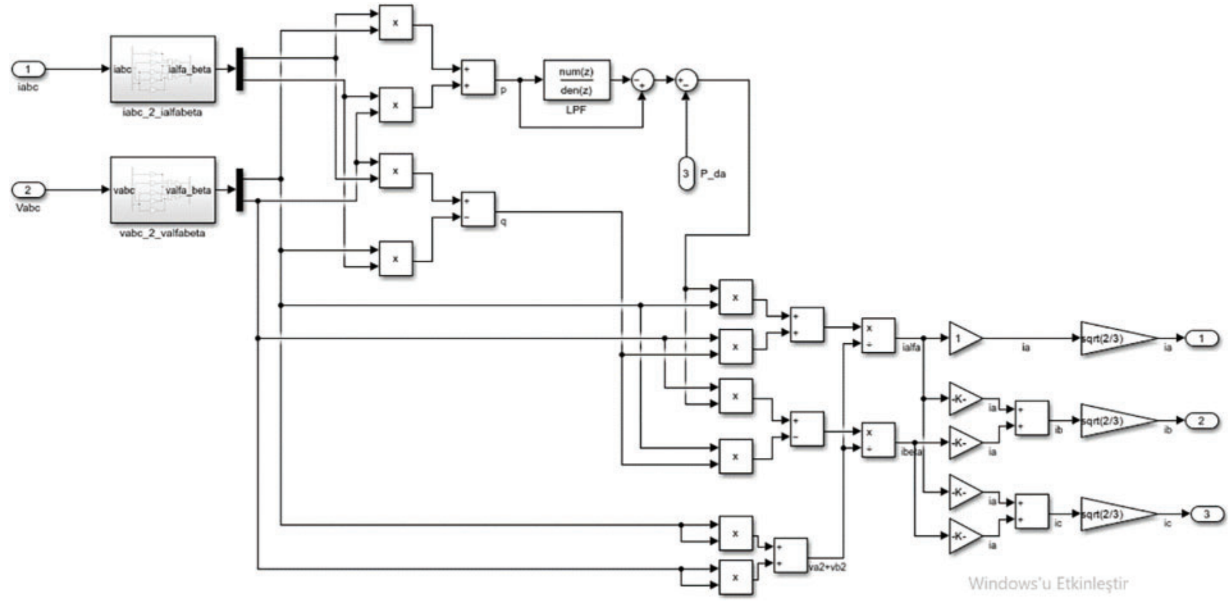

Figure 8: Reference current calculation Matlab/Simulink model of parallel active power filter

The active power filter supplies the harmonic currents in the opposite direction that it generates to suppress the grid harmonics from the DC line capacitor at the input of the three-phase inverter. Therefore, keeping the voltage of this capacitor constant is critical for the AGF to fulfill its function. The PI controller is used for voltage control of the DC line capacitor. K_p and K_i coefficients were set as $K_p = 20$ and $K_i = 15$ by trial and error method. Fig. 9 shows the PI controller of the DC line capacitor.

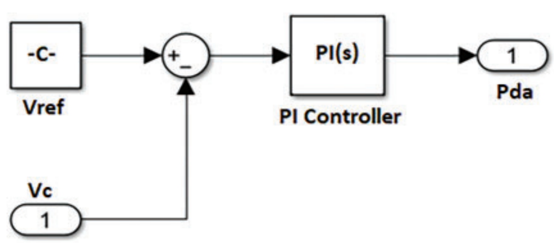

Figure 9: Direct current line capacitor PI controller

2.4.1 *Complete Parallel Active Power Filter Model*

The designed parallel active power filter and nonlinear load model are connected to the power system, and a simulation model is created, as shown in Fig. 10. In the simulation model, circuit breakers are added to the system to adjust the activation time of the parallel active power filter.

3 Result and Discussion

In this study, when the currents drawn in transformer 1, transformer 2, transformer 3, and transformer 4 are analyzed, it is determined that the phase currents are unbalanced. Therefore, the highest current phase is taken as a reference, and a solution is investigated by assuming that the three-phase system is balanced loaded.

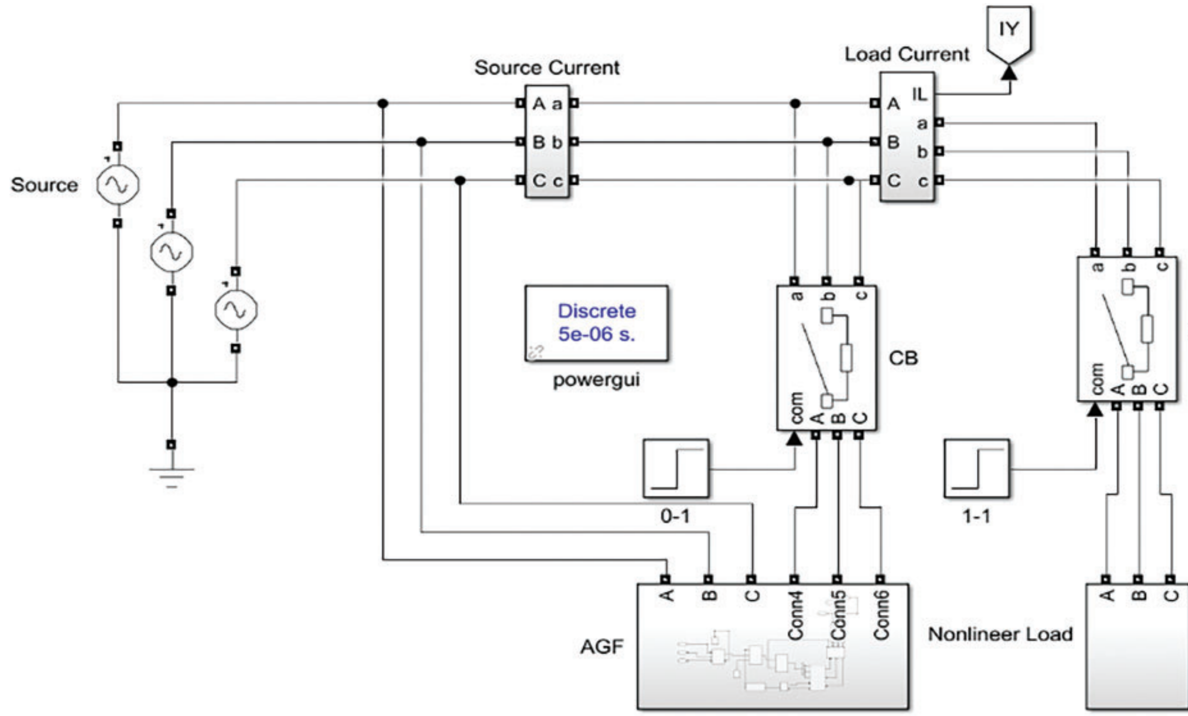

Figure 10: Parallel active power filter complete model

3.1 Transformer 1 (Main Input Transformer) LVF Application

The total harmonic distortion graph and total harmonic distortion ratios (THD) of Transformer 1 with Chauvin Arnoux CA:8331 energy analyzer are given in Fig. 11. When the graph is analyzed, it is seen that voltage harmonics are low, i.e., below the standard limits, while current harmonics are above the standard limits. These differences can also be seen in the graphs of Transformer 2, Transformer 3, and Transformer 4 in Appendix A.

The currents drawn from transformer 1 are given in Table 1. In Appendix A, Transformer 2 current values are given in Appendix B-Table A1 and Fig. A1. The harmonic load model was created according to the current values in Appendix B-Table A1, and it was observed that the phase currents were balanced in the simulations. The current values of transformer 3 are given in Appendix A-Fig. A2 and Appendix B-Table A2. When the values in Appendix B-Table A2 are analyzed, it is determined that transformer 3 has the highest load imbalance compared to other transformers with unbalanced interphase currents. As applied in other transformers, a non-linear load model was created from the current values measured with the energy analyser in transformer 3. When Fig. A3 in Appendix A, i.e., the Transformer 4 THD graph, is examined, since the current harmonics are above the standard limits, the nonlinear load model was obtained by collecting current sources with different amplitudes and frequencies. The measured current values of Transformer 4 are given in Table A3 in Appendix B.

According to the values in this table, current harmonics are combined and nonlinear load model is obtained as shown in Fig. 12.

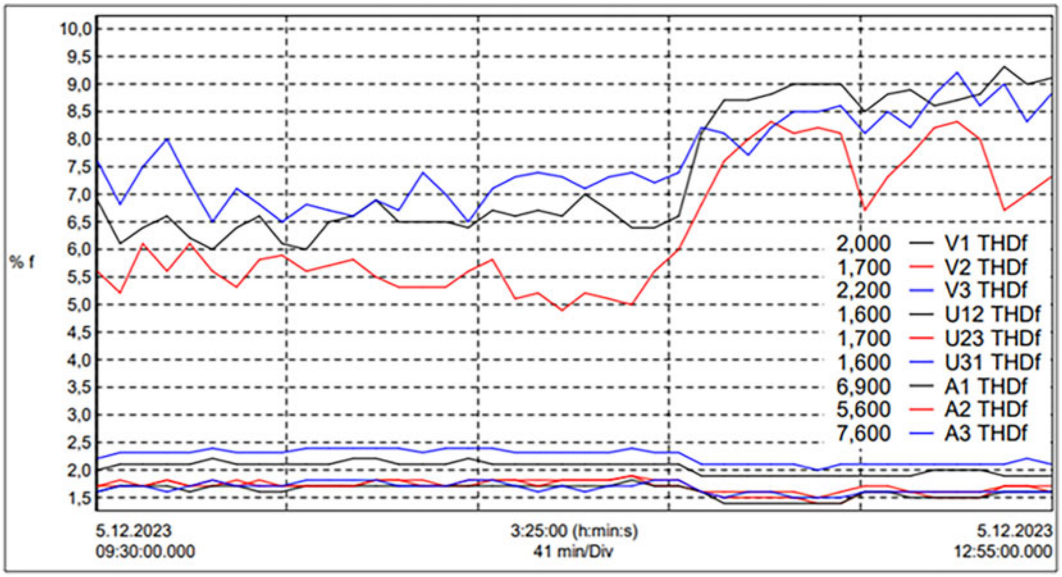

Figure 11: Total harmonic distortion (THD) graph for transformer 1

Table 1: Transformer 1 current values

TR 1	1.H	3.H	5.H	7.H	9.H	11.H	13.H
A_1	407.5	21.64	16.74	2.859	0.816	2.449	2.042
A_2	384.6	17.73	8.479	2.670	4.239	3.855	1.930
A_3	379.8	26.99	7.615	3.045	0.759	3.807	1.903

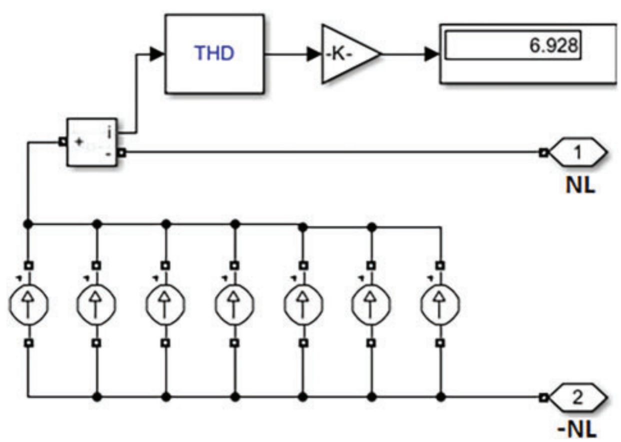

Figure 12: Nonlinear load model created with current sources

In transformer 1, the load current, filter current, and grid current during the simulation period are plotted, respectively, as shown in Fig. 13. The load current, filter current, and grid current for transformer 2, transformer 3, and transformer 4 are also plotted in Appendix B. Initially, the parallel active power filter is not activated. The parallel active power filter is activated after 0.02 s. When the graphs are analyzed, the distortion in the current waveform is seen when the parallel active power filter is not activated. After the activation of the parallel active power filter, the current waveforms drawn from the grid approached the ideal sinusoidal, and the parallel active power filter filtered the current harmonics to a great extent. The same simulation as in Appendix C was performed for Transformer 2, in Fig. A4, Transformer 3, in Fig. A5, and Transformer 4 in Fig. A6. According to these measured values, current sources were connected in parallel, and a nonlinear load model was obtained. When the current values are analyzed, it is understood that the inter-phase currents are unbalanced, and the inter-phase load distribution in transformer 4 in Appendix C should be rearranged. Unbalanced load distribution in three-phase systems causes overheating of transformers, decreased efficiency, and excessive neutral currents.

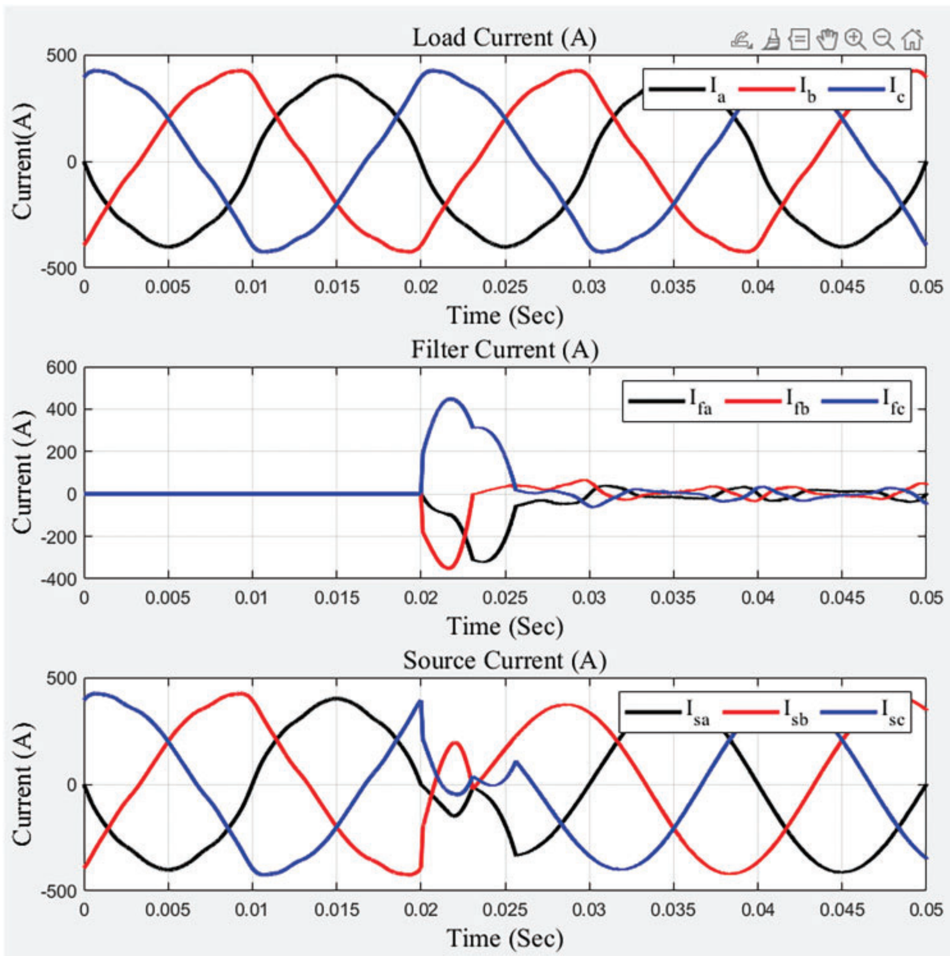

Figure 13: Graph of load current, filter current, and grid load current at transformer 1

Transformer 1 (Fig. 14) shows the Fast Fourier Transform (FFT) analysis graph. This graph shows the current THD when the parallel active power filter is not activated. The THD_I value is calculated as 6.77% when the parallel active power filter is not activated. In addition to the fundamental frequency, 3rd (150 Hz) and 5th (250 Hz) harmonics are dominant compared to other harmonics. Appendix D-Fig. A7 shows that the 5th harmonic is dominant over other harmonics in Transformer 2, and the

THD_I ratio is 5.2% when the parallel active power filter is not activated. The THD_I ratio of transformer 3 in Appendix D-Fig. A8 is 4.60%. In Fig. 14, it is seen from the frequency spectrum that the 3rd harmonic is dominant compared to other harmonics. In Appendix D-Fig. A9, it is determined that the 3rd, 5th, and 7th harmonics are dominant in transformer 4. The THD_I ratio was calculated as 5.64% when the parallel active power filter was not activated.

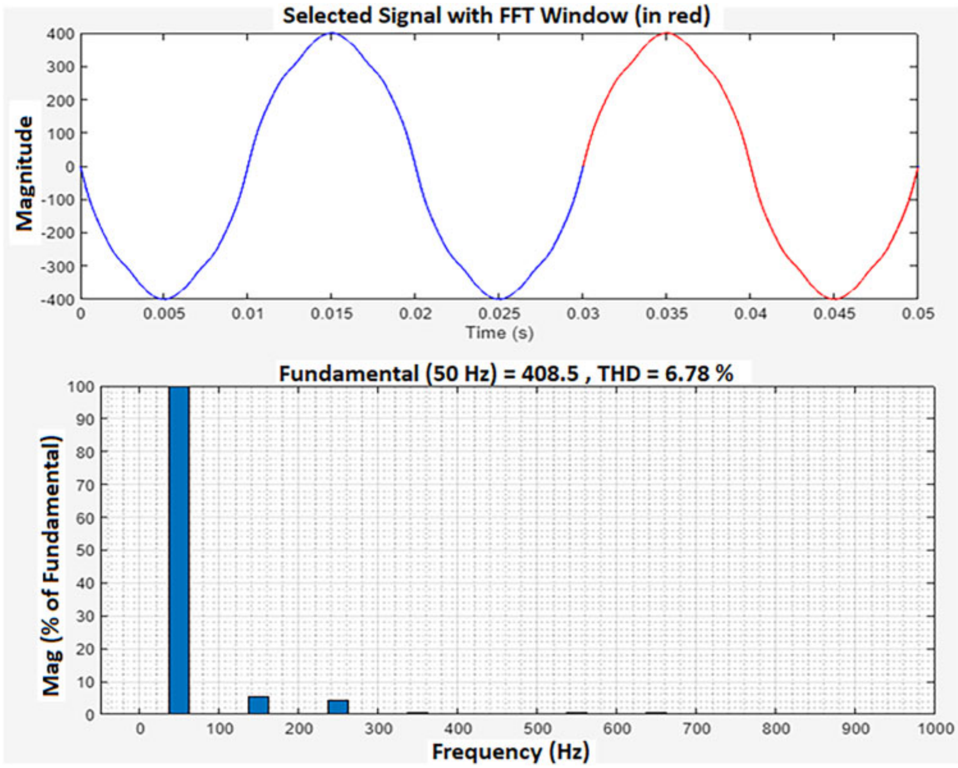

Figure 14: Fast fourier transformation graph at transformer 1

The fast Fourier transform analysis graph after the parallel active power filter is activated is given in Fig. 15. While the THD_I ratio was 6.77% in the fast Fourier transform analysis when the parallel active power filter was not activated, this ratio decreased to 1.37% after the parallel active power filter was activated. Appendix E-Fig. A10 shows that the THD_I ratio decreased to 2.21%. In Appendix E-Fig. A11, THD_I decreased from 4.60% to 1.41%. The 3rd harmonic, which was dominant when the parallel active power filter was not activated, was completely suppressed after the parallel active power filter was activated. In the same way, in Appendix E-Fig. A12, the fast Fourier transform graph of Transformer 4 with a parallel active power filter is given.

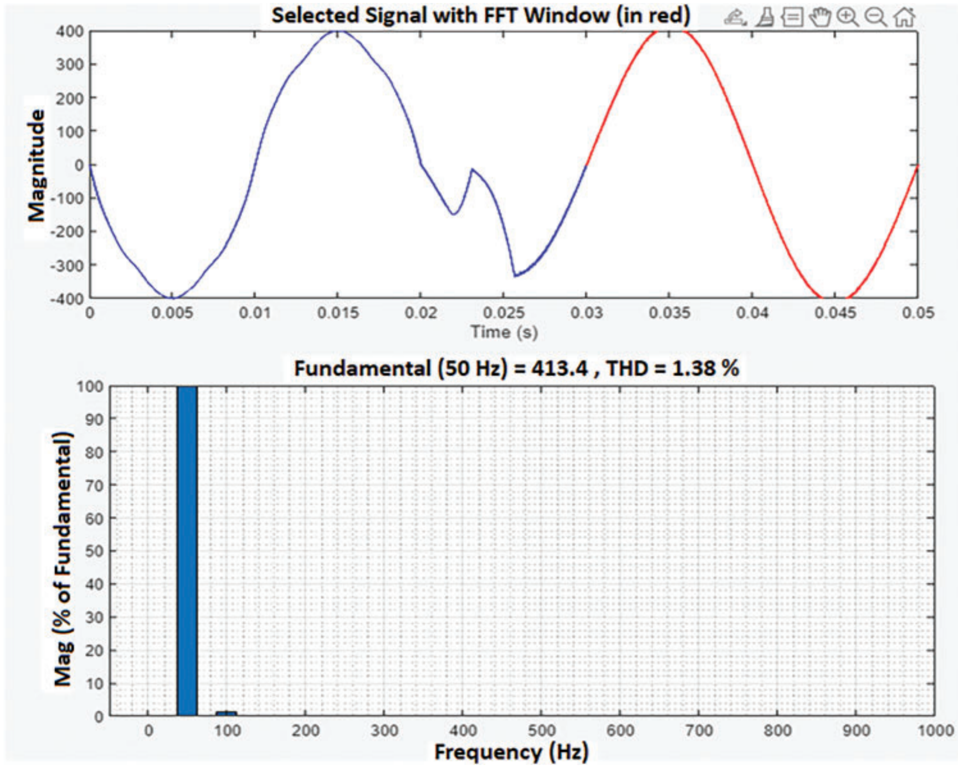

Figure 15: Fast fourier transform graph for transformer 1 with parallel active power filter activated

4 Discussion

During the generation, transmission, and distribution of energy in electrical power systems, current and voltage are required to be at a frequency of 50 Hz and in a form very similar to the sine curve. This condition is one of the main factors determining the quality of electrical energy. However, due to the harmonics produced by nonlinear loads, quantities such as flux, current, and voltage cease to be sinusoidal, and their waveforms become quite complex. As a result, significant problems arise that are not desirable for operation. In high current installations, oversaturated transformers, arc furnaces, arc welding machines, electric machines, and power electronics elements, which are nowadays highly developed, cause harmonics to occur in the network. Compensation facilities have gained importance and become widespread with the realisation of the damage to the national economy caused by the network being loaded with a low power factor. This can cause harmonics to cause damage to the capacitors used in compensation facilities in resonance and perforation of insulating cables and constitutes a major problem. The negative effects of harmonics in the energy system can be divided into two categories: technical and economic problems. Technical problems are the problems that adversely affect the operation of the system and prevent the provision of quality energy to the consumer. Economic problems are the problems caused by the additional losses caused by harmonics in the system. The absence of harmonics provides a great benefit for energy systems. However, it is seen that this is not possible under today's conditions. Therefore, the effects of harmonics can be considered to be reduced or even eliminated. There are two methods for this: one is to design the device in such a way that it does not produce harmonics or produces harmonics at a low level, and the other is to remove harmonics from the system by filtering them through filters. In this study, current and voltage harmonics were recorded by connecting an energy analyzer to the transformers on campus to create a nonlinear load model. When the recorded current and voltage harmonics were analyzed, it was determined that the THD_V ratios of voltage harmonics were below the limits specified in the standards, while the THD_I ratios of currents were higher than the limits specified in the standards. In order to model the current harmonics measured from the transformers, current sources were connected in parallel in the Matlab/Simulink program, and THD values close to the actual measured current harmonics were obtained from the current harmonics up to the tenth harmonic. As a result of this study, the THD_I ratio decreased from 6.78% to 1.38% in the fast Fourier transform analyses performed after the parallel active power filter was activated in the first transformer. Similarly, the THD_I ratio decreased from 5.2% to 2.21% in the second transformer, from 4.6% to 1.41% in the third transformer, and from 5.64% to 1.37% in the fourth transformer. During the generation, transmission, and distribution of energy in electrical power systems, the current and voltage are required to be at a frequency of 50 Hz and in a form very similar to the sine curve. This condition is one of the main factors determining the quality of electrical energy. However, due to the harmonics produced by nonlinear loads, quantities such as current and voltage cease to be sinusoidal, and their waveforms become quite complex. As a result, significant problems arise that are not desirable for operation. In this study, in a plant with a laser lathe, in a plant with a computer numeric control (CNC) vertical lathe, and in a plant with an induction melting furnace, parameters such as current, voltage, and power of the system were recorded with a power analyzer. The data obtained were transferred to the computer, and power analysis was performed. In the analyses, current and voltage harmonics were examined, and the losses caused by current and voltage harmonics in the system were calculated. In the studies of [59], it is seen that there are serious losses in the system in percentage (34.03%) as a result of harmonics and that the harmonics reduction studies should be implemented as soon as possible as published in the official gazette. As a result, the parallel active power filter in the design used in our study has successfully filtered current harmonics. However, passive power filter design can also be made according to the dominant harmonics by making harmonic measurements for long-term and various load conditions [60].

5 Conclusion

In this study, the transformers at Muş Alparslan University campus were analyzed for current and voltage harmonics, and a parallel active power filter was designed to mitigate the measured harmonics. The measurements revealed that the voltage harmonics were within the standard limits, while the current harmonics exceeded the allowable thresholds. To generate the reference current, instantaneous power theory was applied. Instantaneous active and reactive powers were calculated using this theory, and the harmonic component of the instantaneous active power was determined by subtracting the 50 Hz fundamental frequency power from the total instantaneous active power. The three-phase reference currents were derived from the biaxial currents, and these were fed into a hysteresis band controller to regulate the parallel active power filter. The DC line voltage of the voltage source inverter was controlled using a PI controller. For the nonlinear load model, current sources were connected in parallel based on the current values measured with the energy analyzer. Load models were created separately for each transformer, and simulations of the parallel active power filter were performed in Matlab/Simulink for each transformer (transformers 1, 2, 3, and 4). In the simulations, the parallel active power filter was initially inactive and was activated at 0.02 s. After activating the filter in the first transformer, the total harmonic distortion current (THD_I) ratio decreased from 6.78% to 1.38% based on fast Fourier transform analysis. Similarly, the THD_I ratio in the second transformer decreased from 5.1% to 2.19%, from 4.5% to 1.39% in the third transformer, and from 5.63% to 1.36% in the fourth transformer. These results demonstrate a significant reduction in the harmonic currents drawn from the grid by the nonlinear load. After activating the parallel active power filter, the current waveforms drawn from the grid were significantly improved and closely aligned with the ideal sine wave, effectively suppressing the harmonic distortions. In addition, harmonic currents cause extra losses and heating in transformers and transmission lines. When the parallel active power filter is switched on, THD_I is reduced, and system losses are significantly reduced. This improves the overall efficiency of the electrical system, resulting in lower energy consumption and longer equipment life. Harmonics and load imbalances are important for voltage stability, but voltage harmonics are not included in the study since they are within the standards. Concerning the power factor, harmonics increase the reactive current due to inductive loads. As a result of the suppression of harmonic currents, the total currents drawn from the network decrease, the reactive currents decrease, and the system efficiency increases. In the measurements made together with the harmonic measurements, it can be determined that the loading in the phases is unbalanced, and this may cause neutral currents to be drawn and unbalanced in harmonic voltages. It was observed that harmonic voltage stabilization was performed and that interharmonics around the harmonic frequencies that do not correspond to an integer have a negative effect and should be eliminated. Power quality is one of the most important problems in the power system. Harmonic studies and harmonic filtering with passive power filters are not sufficient to prevent the effects of nonlinear loads on power quality. Therefore, an active power filter comes into play. Although passive filters offer a low-cost solution by suppressing certain harmonic components, they may cause resonance problems. In addition, they may not provide the desired performance under variable load conditions. Besides, active power filters have wider band harmonic suppression capabilities and can adapt to dynamic load conditions. However, active filters are economically disadvantageous due to high switching losses and initial investment costs. As a result, the presence of harmonics does not mean that electrical systems will not work. Considering that the filter itself is also a source of harmonics, it shows that these sensitivities should be taken into account in the design process.

Acknowledgement: None.

Funding Statement: The authors received no specific funding for this study.

Author Contributions: The authors confirm contribution to the paper as follows: Methodology, Sabir Rüstemli, Nejdet Sezgin, Bilal Coşkun, Gökhan Şahin; Software, Sabir Rüstemli, Nejdet Sezgin, Bilal Coşkun, Gökhan Şahin; Formal analysis, Sabir Rüstemli, Nejdet Sezgin, Bilal Coşkun, Gökhan Şahin; Investigation, Sabir Rüstemli, Nejdet Sezgin, Bilal Coşkun, Gökhan Şahin; Writing original draft, Methodology, Sabir Rüstemli, Nejdet Sezgin, Bilal Coşkun, Gökhan Şahin; Writing—review & editing, Gökhan Şahin. All authors reviewed the results and approved the final version of the manuscript.

Availability of Data and Materials: The datasets generated and/or analyzed during the current study are available from the corresponding author upon reasonable request.

Ethics Approval: Not applicable.

Conflicts of Interest: The authors declare no conflicts of interest to report regarding the present study.

References

1. Izhar M, Hadzer CM, Masri S, Idris S. A study of the fundamental principles to power system harmonic. In: Proceedings of the National Power Engineering Conference 2003; 2003 Dec 15–16; Bangi, Malaysia.
2. León-Martínez V, Peñalvo-López E, Montañana-Romeu J, Andrada-Monrós C, Molina-Cañamero L. Assessment of load losses caused by harmonic currents in distribution transformers using the transformer loss calculator software. Environments. 2023;10(10):177. doi:10.3390/environments10100177.
3. Chen H, Huang Y, Hu H, Wang J, Wang W. Analysis of the influence of voltage harmonics on the maximum load capacity of the power supply transformer for the LHCD system. In: Proceedings of the 2023 IEEE 6th International Electrical and Energy Conference (CIEEC); 2023 May 12–14; Hefei, China.
4. Mikhak-Beyranvand M, Faiz J, Rezaeealam B. Thermal analysis and derating of a power transformer with harmonic loads. IET Gener Transm Distrib. 2020;14(7):1233–41. doi:10.1049/iet-gtd.2019.0703.
5. Yaghoobia J, Alduraibia A, Martina D, Zarea F, Eghbalc D, Memisevic R. Impact of high-frequency harmonics (0–9 kHz) generated by grid-connected inverters on distribution transformers. Electr Power Energy Syst. 2020;122(2):106177. doi:10.1016/j.ijepes.2020.106177.
6. Şahin G, Angay MN, Rustemli S, van Sark W. Study on the capacitive effects of underground power cables on the operational electricity distribution network. Electr Power Compon Syst. 2024;2023(2):1–20. doi:10.1080/15325008.2023.2300327.
7. Sainz L, Pedra J, Mesas JJ. Single- phase full-wave rectifier study with experimental measurements. Electr Power Syst Res. 2007;77(3–4):339–51. doi:10.1016/j.epsr.2006.03.010.
8. Bao M, Xıa J, Yın X, Dong M, He H, He J. Harmonic measurements and analysis in a modern steel manufacturing facility. In: Proceedings of the IEEE PES General Meeting; 2010 Jul 25–29; Minneapolis, MN, USA.
9. Tang Q, Wang Y, Guo S. Design of power system harmonic measurement system based on LabVIEW. In: Proceedings of the 2008 Fourth International Conference on Natural Computation; 2008 Oct 18–20; Jinan, China.
10. Chang GW, Cheng-I C. Measurement techniques for stationary and time-varying harmonics. In: Proceedings of the IEEE PES General Meeting; 2010 Jul 25–29; Minneapolis, MN, USA.
11. Coban M, Saka M. Directly power system harmonics estimation using equilibrium optimizer. Electr Power Syst Res. 2024;234:110565. doi:10.1016/j.epsr.2024.110565.
12. Parvez M, Elias MFM, Rahim NA, Osman N. Current control techniques for three-phase grid interconnection of renewable power generation systems: a review. Sol Energy. 2016;135(2):29–42. doi:10.1016/j.solener.2016.05.029.
13. Velazquez-Ibañez A, Rodríguez-Rodríguez JR, Arrieta-Paternina MR, Segundo-Sevilla FR, Korba P. Definition of safe operating limits for dq control-based voltage source converters under unbalanced grid voltages. Appl Energy. 2024;367(12):123325. doi:10.1016/j.apenergy.2024.123325.
14. Mazin HE, Xu W. Harmonic cancellation characteristics of specially connected transformers. Electr Power Syst Res. 2009;79(2):1689–97. doi:10.1016/j.epsr.2009.07.006.
15. Sepulveda CA, Munoz JA, Espinoza JR, Figueroa ME. All-on-chip DQ-frame based D-STATCOM control implementation in a low-cost FPGA. IEEE Trans Ind Electron. 2013;60(2):659–69. doi:10.1109/TIE.2012.2206353.
16. Zaveri T, Bhalja B, Zaveri N. Load compensation using DSTATCOM in three-phase, three-wire distribution system under various source voltage and delta connected load conditions. Int J Electr Power Energy Syst. 2012;41(1):34–43. doi:10.1016/j.ijepes.2012.02.015.
17. Karmiris G, Tsengenes G, Adamidis G. A multifunction control scheme for current harmonic elimination and voltage sag mitigation using a three phase three level flying capacitor inverter. Simul Model Pract Theory. 2012;24(5):15–34. doi:10.1016/j.simpat.2012.01.007.

18. Solanki J, Frohleke N, Bocker J, Wallmeier P. Analysis, design and control of 1MW, high power factor and high current rectifier system. In: Proceedings of the 2012 IEEE Energy Conversion Congress and Exposition (ECCE); 2012 Sep 15–20; Raleigh, NC, USA.
19. Arya RS, Singh B. Power quality improvement under nonideal AC mains in distribution system. Electr Power Syst Res. 2014;106(1):86–94. doi:10.1016/j.epsr.2013.08.008.
20. Arya SR, Singh B. Performance of DSTATCOM using leaky LMS control algorithm. IEEE J Emerg Sel Top Power Electron. 2013;1(2):104–13. doi:10.1109/JESTPE.2013.2266372.
21. Singh B, Arya SR. Implementation of single-phase enhanced phase-locked loop-based control algorithm for three-phase DSTATCOM. IEEE Trans Power Deliv. 2013;28(3):1516–24. doi:10.1109/TPWRD.2013.2257876.
22. Singh B, Arya SR. Back-propagation control algorithm for power quality improvement using D STATCOM. IEEE Trans Ind Electron. 2014;61(3):1204–12. doi:10.1109/TIE.2013.2258303.
23. Singh B, Arya SR. Composite observer-based control algorithm for distribution static compensator in four wire supply system. IET Power Electron. 2013;6(2):251–60. doi:10.1049/iet-pel.2012.0412.
24. Arya SR, Singh B. Implementation of distribution static compensator for power quality enhancement using learning vector quantisation. IET Gener Transm Distrib. 2013;7(11):1244–52. doi:10.1049/iet-gtd.2012.0689.
25. Singh B, Arya SR, Chandra A, Al-Haddad K. Implementation of adaptive filter based control algorithm for distribution static compensator. In: Proceedings of the 2012 IEEE Industry Applications Society Annual Meeting; 2012 Oct 7–11; Las Vegas, NV, USA.
26. Contreras-Ramirez D, Lata-García J. K-factor analysis to increase the actual capacity of electrical distribution transformers. In: Proceedings of the International Conference on Science, Technology and Innovation for Society (CITIS 2021); 2021 May 26–28; Guayaquil, Ecuador. doi:10.1007/978-981-16-4126-8_34.
27. Arya SR, Singh B, Chandra A, Al-Haddad K. Control of shunt custom power device based on Anti Hebbian learning algorithm. In: Proceedings of the IECON 2012-38th Annual Conference on IEEE Industrial Electronics Society; 2012 Oct 25–28; Montreal, QC, Canada.
28. Plienis M, Deveikis T, Jonaitis A, Gudžius S, Konstantinavi I, Putnaite D. Improved methodology for power transformer loss evaluation: algorithm refinement and resonance risk analysis. Energies. 2023;16(23):7837. doi:10.3390/en16237837.
29. Arya SR, Singh B, Chandra A, A.I.-Haddad K. Control of DSTATCOM using adjustable step least mean square control algorithm. In: Proceedings of the 2012 IEEE Fifth Power India Conference; 2012 Dec 19–22; Murthal, India.
30. Singh B, Solanki J. A comparison of control algorithms for DSTATCOM. IEEE Trans Ind Electron. 2009;56(7):2738–45. doi:10.1109/TIE.2009.2021596.
31. Seddik MS, Eteiba MB, Shazly J. Evaluating the harmonic effects on the thermal performance of a power trans-former. Energies. 2024;17(19):4871. doi:10.3390/en17194871.
32. Shukla A, Joshi A. State feedback control of multilevel inverters for DSTATCOM applications. IEEE Trans Power Deliv. 2007;22(4):2409–18. doi:10.1109/TPWRD.2007.905271.
33. Singh B, Jayaprakash P, Kothari DP. New control approach for capacitor supported DSTATCOM in three-phase four wire distribution system under non ideal supply voltage conditions based on synchronous reference frame theory. Int J Electr Power Energy Syst. 2011;33(5):1109–17. doi:10.1016/j.ijepes.2010.12.006.
34. Aggarwal M, Gupta SK, Singh M. Analysis and control of grid connected wind energy system with DSTATCOM. In: Proceedings of the 2012 IEEE Fifth Power India Conference; 2012 Dec 19–22; Murthal, India.
35. Elnady A, Salama MMA. Unified approach for mitigating voltage sag and voltage flicker using the DSTATCOM. IEEE Trans Power Deliv. 2005;20(2):992–1000. doi:10.1109/TPWRD.2004.837670.

36. Rudi FS, Hashemnia MN. Compensation of active filter using p-q theory in photovoltaic systems. Mem-Mater Devices Circuits Syst. 2025;9(1):100122. doi:10.1016/j.memori.2025.100122.
37. Guerrero-Rodríguez NF, Nuñez-Ramíre V, Batista-Jorge RO, Mercado-Ravelo R, Ramírez-Rivera FA, Ferreira JA, et al. Modelling real non-linear loads for a controller hardware-in-the-loop configuration to evaluate a shunt active power filter. Energy Rep. 2024;12(3):1947–76. doi:10.1016/j.egyr.2024.07.056.
38. Efe SB, Kocaman B. Harmonic analysis of a wind energy conversion system with small-scale wind turbine. Int J Energy Appl Technol. 2018;5(4):168–73. doi:10.31593/ijeat.441563.
39. Rustemli S, Satici MA, Şahin G, van Sark W. Investigation of harmonics analysis power system due to non-linear loads on the electrical energy quality results. Energy Rep. 2023;10(1):4704–32. doi:10.1016/j.egyr.2023.11.034.
40. Kuwalek P, Wiczyński G. Laboratory setup for testing low-frequency disturbances of power quality. In: Proceedings of the 2024 IEEE 18th International Conference on Compatibility, Power Electronics and Power Engineering (CPE-POWERENG); 2024 Jun 24–26; Gdynia, Poland. doi:10.1109/CPE-POWERENG60842.
41. Wakileh GJ. Power systems harmonics: fundamentals, analysis and filter design. Berlin/Germany: Springer Nature; 2019. 517 p.
42. Harmonics PS. Power system harmonics: an overview. IEEE Trans Power Appar Syst. 1993;8:2455–60.
43. Imam AA, Kumar RS, Al-Turki YA. Modeling and simulation of a PI controlled shunt active power filter for power quality enhancement based on P-Q theory. Electronics. 2020;9(4):637. doi:10.3390/electronics9040637.
44. Mustafa S, Melih C. Harmonic estimator design using improved gazelle optimization algorithm by chaos for real field signal. Expert Syst Appl. 2025;267:2–15.
45. Jia W, Wang C, Xiang J. A novel approach to estimating harmonic/interharmonic parameters. Measurement. 2025;240(13):2–10. doi:10.1016/j.measurement.2024.115586.
46. Serov V. Fourier series, fourier transform and their applications to mathematical physics, Vol. 197. Berlin/Heidelberg, Germany: Springer Nature; 2017.
47. Grady WM, Santoso S. Understanding power system harmonics. IEEE Power Eng Rev. 2001;21(11):8–11. doi:10.1109/MPER.2001.961997.
48. Arrillaga J, Watson NR. Power system harmonics. Hoboken, NJ, USA: John Wiley & Sons, Inc.; 2003.
49. Cheema KM, Mehmood K, Chaudhary NI, Khan ZA, Raja MAZ, El-Sherbeeny AM, et al. Knacks of marine predator heuristics for distributed energy source-based power systems harmonics estimation. Heliyon. 2024;10(15):e35776. doi:10.1016/j.heliyon.2024.e35776.
50. Peng FZ, Huang H, Tolbert LM, Lehman B, Li YA. Spacetime pq theory for AC and DC electric power systems. Sci Rep. 2025;15(1):8169. doi:10.1038/s41598-025-90021-3.
51. Motta L, Faundes N. Active/passive harmonic filters: applications, challenges & trends. In: Proceedings of the 2016 17th International Conference on Harmonics and Quality of Power (ICHQP); 2016 Oct 16–19; Belo Horizonte, Brazil.
52. Badrzadeh B, Smith KS, Wilson RC. Designing passive harmonic filters for an aluminum smelting plant. IEEE Trans Ind Appl. 2011;47(2):973–83. doi:10.1109/TIA.2010.2103544.
53. Rüstemli S, Kocaman Y, Kocaman B, Şahin G, van Sark W. The effect of using automatic meter reading system in electricity distribution systems on reducing non-technical losses: the case of Bitlis province in Turkey. Energy Strategy Rev. 2025;58(1):101674. doi:10.1016/j.esr.2025.101674.
54. Michalec L, Jasiński M, Sikorski T, Leonowicz Z, Jasiński Ł, Suresh V. Impact of harmonic currents of non-linear loads on power quality of a low voltage network-review and case study. Energies. 2021;14(12):3665. doi:10.3390/en14123665.

55. Ruviaro A, Sperandio M, Ebert P, Boaski MAF, Mallmann JF. Energy efficiency studies in a Brazilian university campus. In: Proceedings of the 2018 IEEE PES Transmission & Distribution Conference and Exhibition-Latin America (T&D-LA); 2018 Oct 18–21; Lima, Peru.
56. Akagi H, Watanabe EH, Aredes M. Instantaneous power theory and applications to power conditioning. Hoboken, NJ, USA: John Wiley & Sons, Inc.; 2017. 389 p.
57. Uddin N, Khallil ME, Das TK, Sarker S. Evaluation of active filter design and harmonics analysis using MATLAB. In: Proceedings of the 2021 International Conference on Automation, Control and Mechatronics for Industry 4.0 (ACMI); 2021 Jul 8–9; Rajshahi, Bangladesh.
58. Nishad DK, Tiwari AN, Khalid S, Gupta S, Shukla A. AI-based UPQC control technique for power quality optimization of railway transportation systems. Sci Rep. 2024;14(1):17935. doi:10.1038/s41598-024-68575-5.
59. Brasil VP, Ishihara JY, Ferreira Filho ADL. Investigating power factor definitions in the context of unbalanced loads and voltages. IEEE Trans Power Deliv. 2024;39(4):2340–55. doi:10.1109/TPWRD.2024.3403040.
60. Blooming TM, Carnovale DJ. Application of IEEE STD 519-1992 harmonic limits. In: Proceedings of the Conference Record of 2006 Annual Pulp and Paper Industry Technical Conference; 2006 Jun 18–23; Appleton, WI, USA. doi:10.1109/PAPCON.2006.1673767.

Appendix A

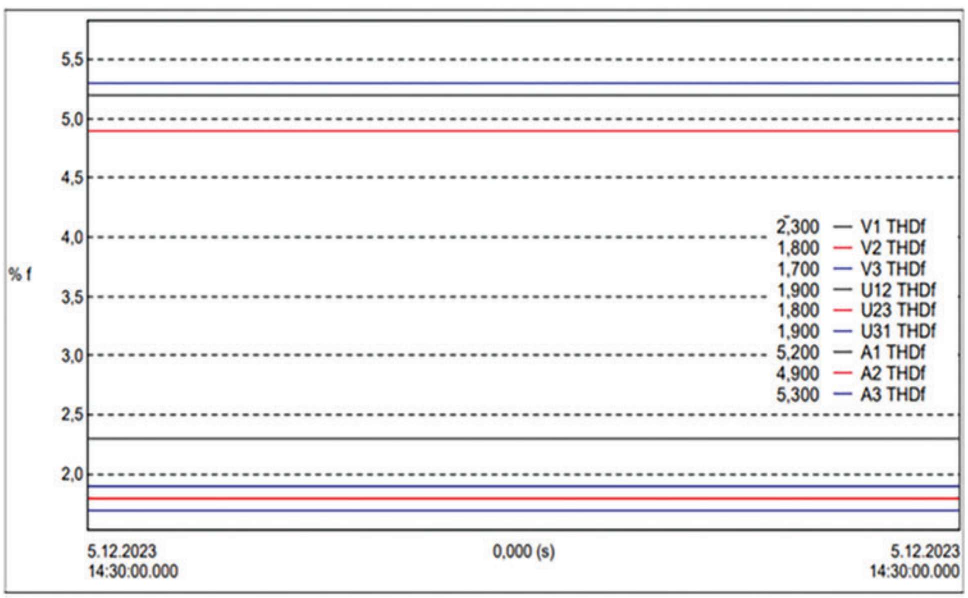

Figure A1: THD graph for transformer 2

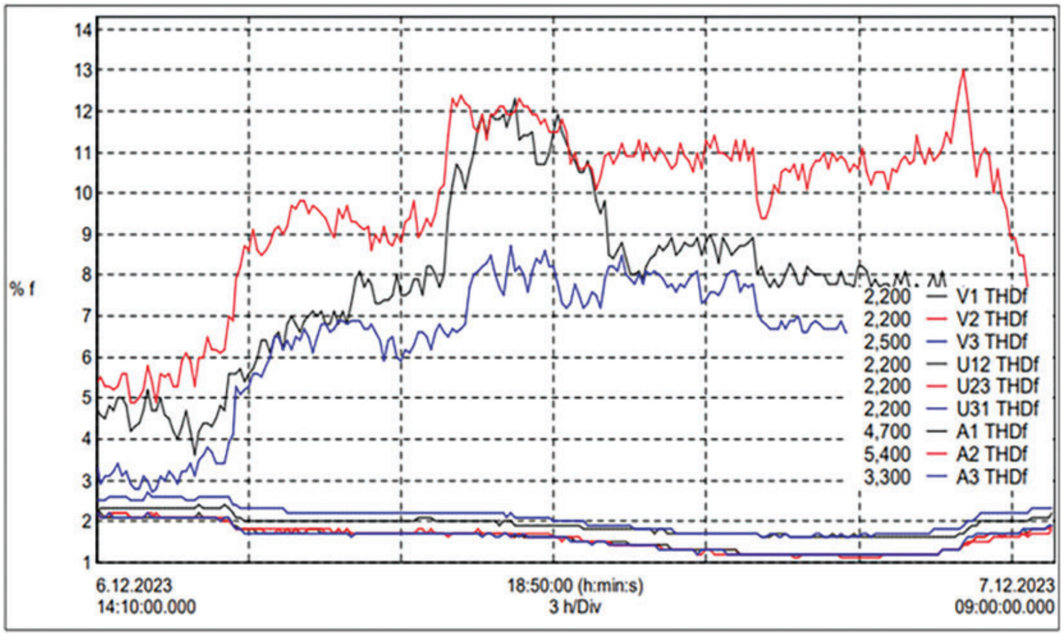

Figure A2: Transformer 3 THD graph

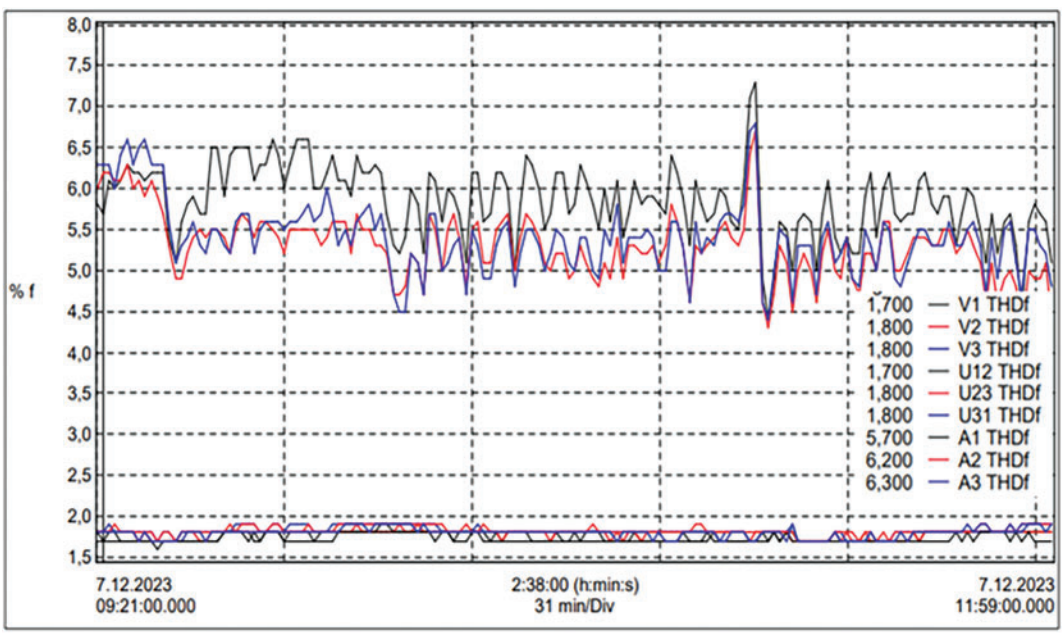

Figure A3: Transformer 4 THD graph

Appendix B

Table A1: Transformer 2 current values

TR 2	1.H	3.H	5.H	7.H	9.H	11.H	13.H
A_1	169.19	2.029	8.459	1.353	0.001	0.001	0.170
A_2	162.09	1.784	7.458	1.134	0.487	0.163	0.163
A_3	174.69	3.320	8.387	1.397	0.350	0.174	0.174

Table A2: Transformer 3 current values

TR 3	1.H	3.H	5.H	7.H	9.H	11.H	13.H
A_1	372.9	15.98	3.729	4.479	0.373	0.748	1.495
A_2	306.8	13.01	6.769	6.769	1.229	0.616	1.538
A_3	272.0	7.369	1.637	1.910	0.545	0.818	0.818

Table A3: Transformer 4 current values

TR 4	1.H	3.H	5.H	7.H	9.H	11.H	13.H
A_1	405.59	9.733	17.03	11.35	1.216	1.623	2.029
A_2	393.29	8.260	19.68	10.63	2.359	2.754	1.968
A_3	338.89	11.87	14.90	8.474	2.030	2.373	2.034

Appendix C

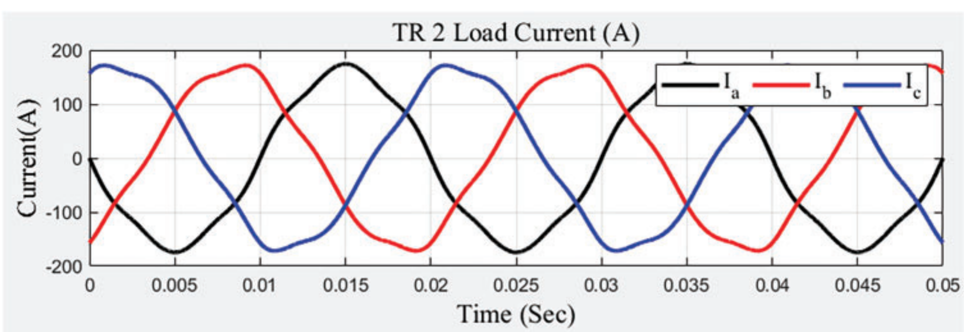

Figure A4: (Continued)

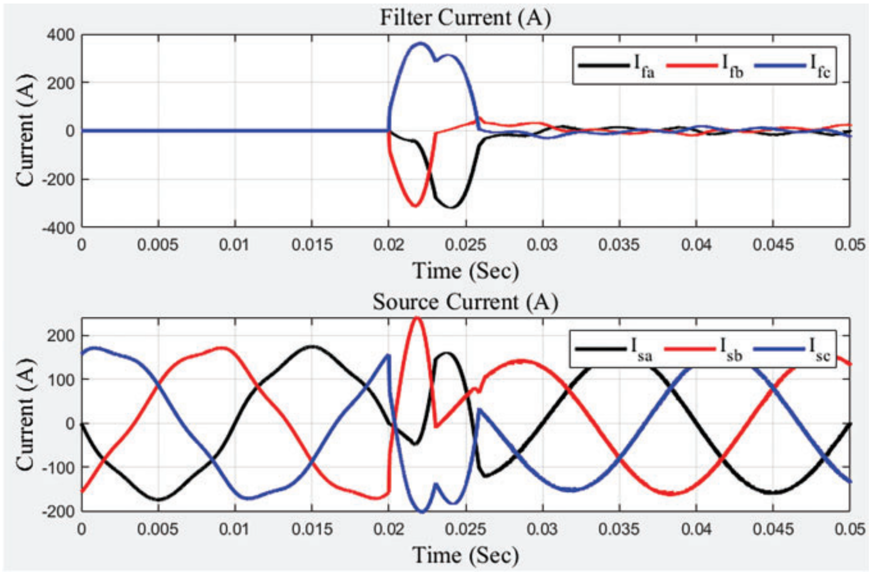

Figure A4: Graph of load current, filter current, grid load current at transformer 2

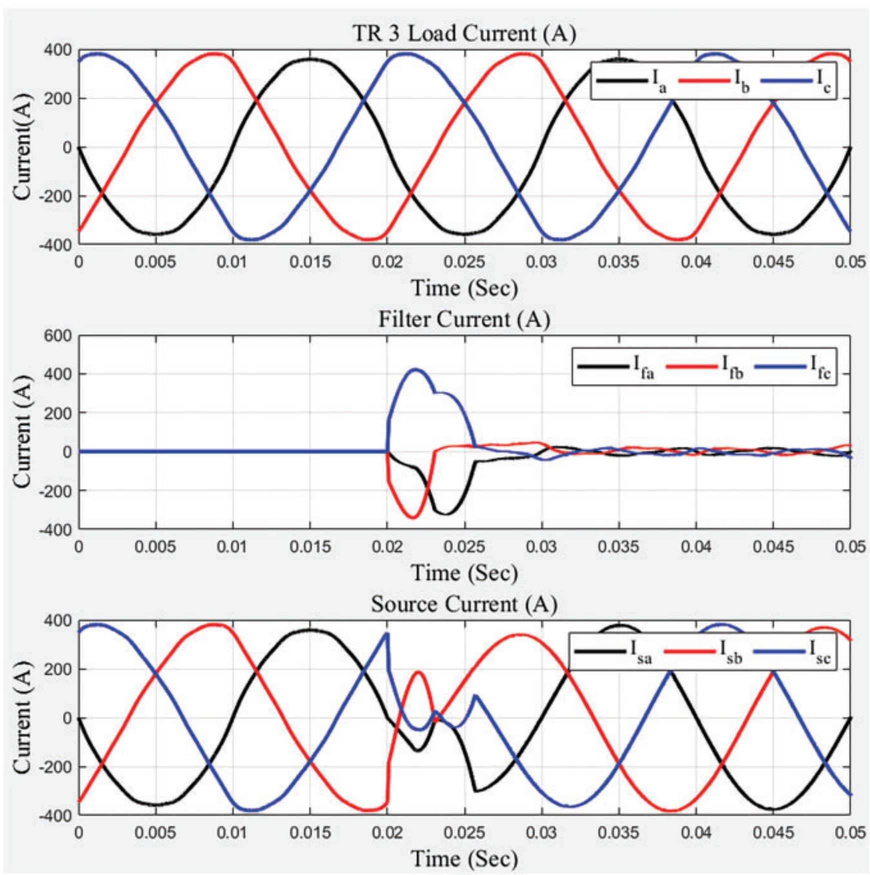

Figure A5: Graph of load current, filter current, grid load current at transformer 3

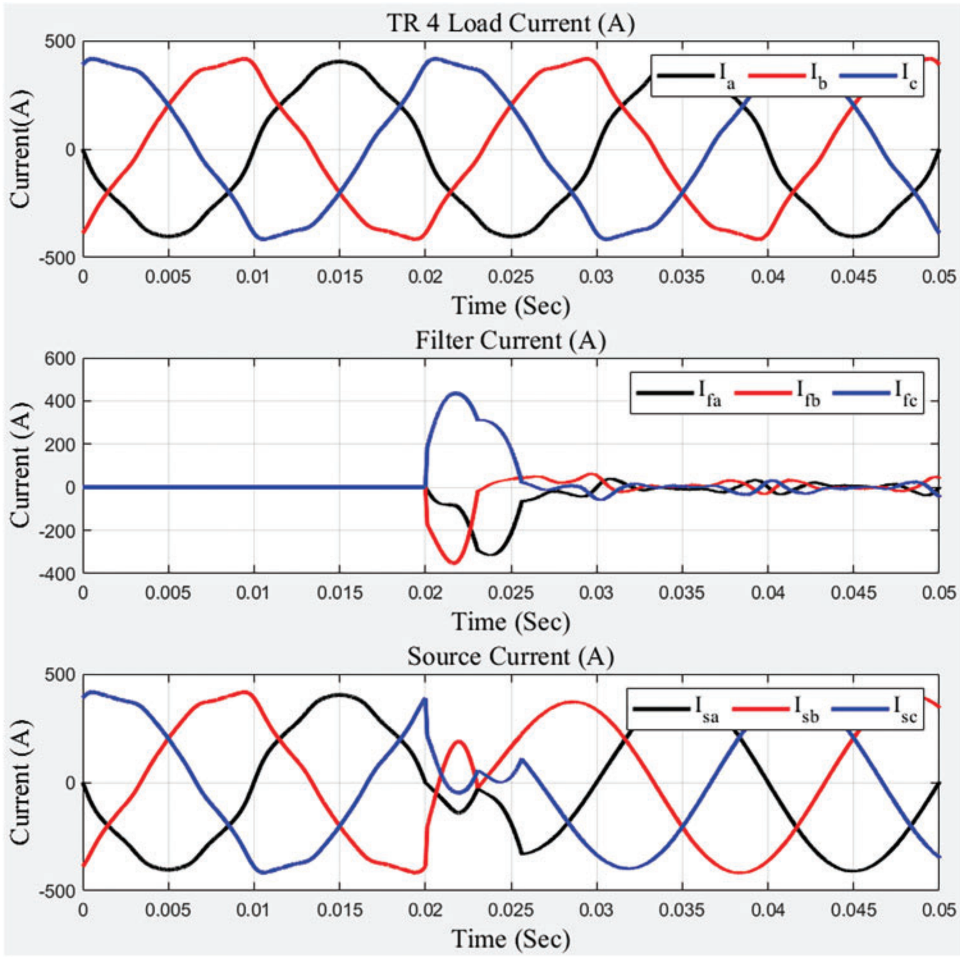

Figure A6: Graph of load current, filter current, grid load current at transformer 4

Appendix D

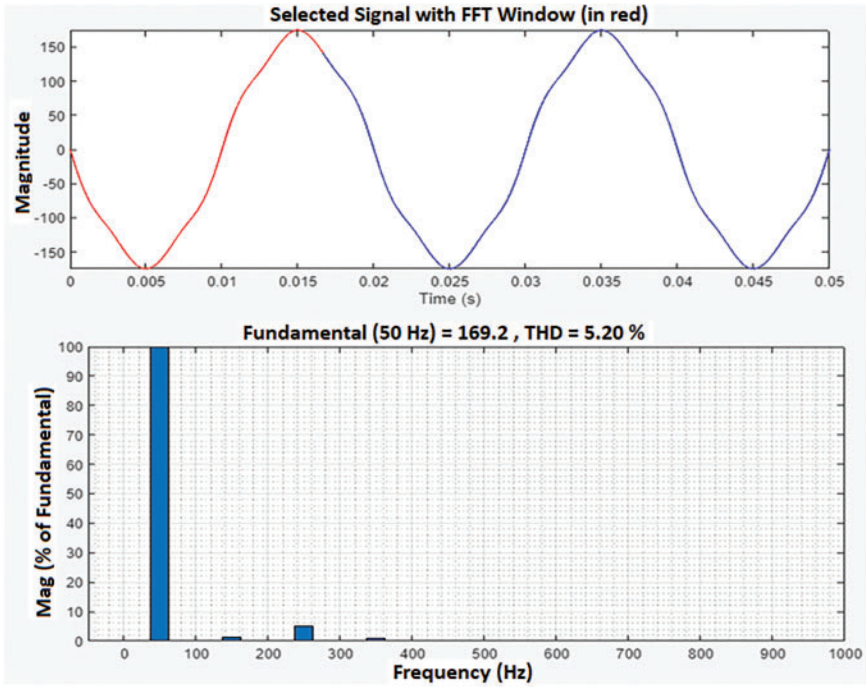

Figure A7: Fast fourier transformation graph at transformer 2

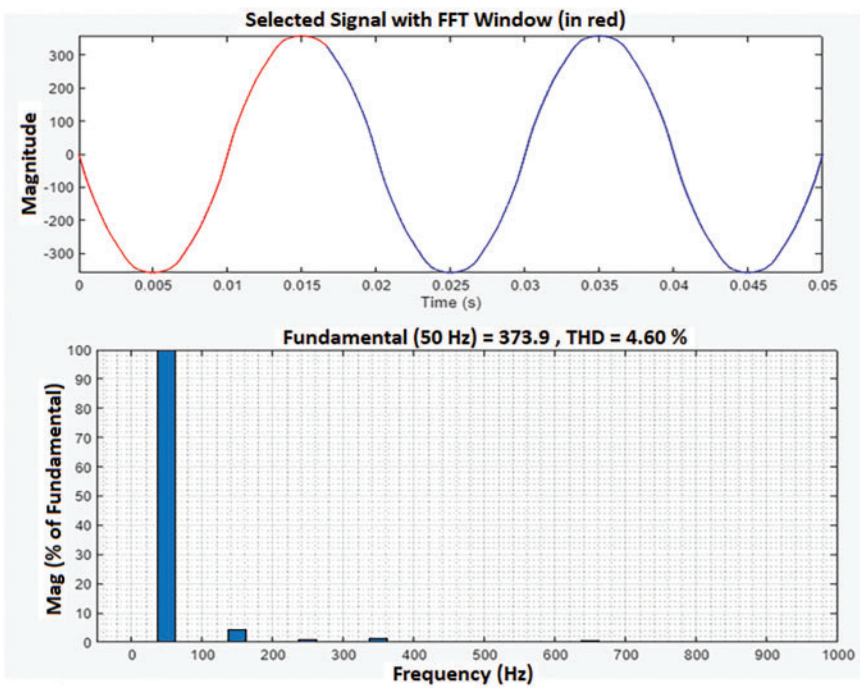

Figure A8: Fast fourier transformation graph at transformer 3

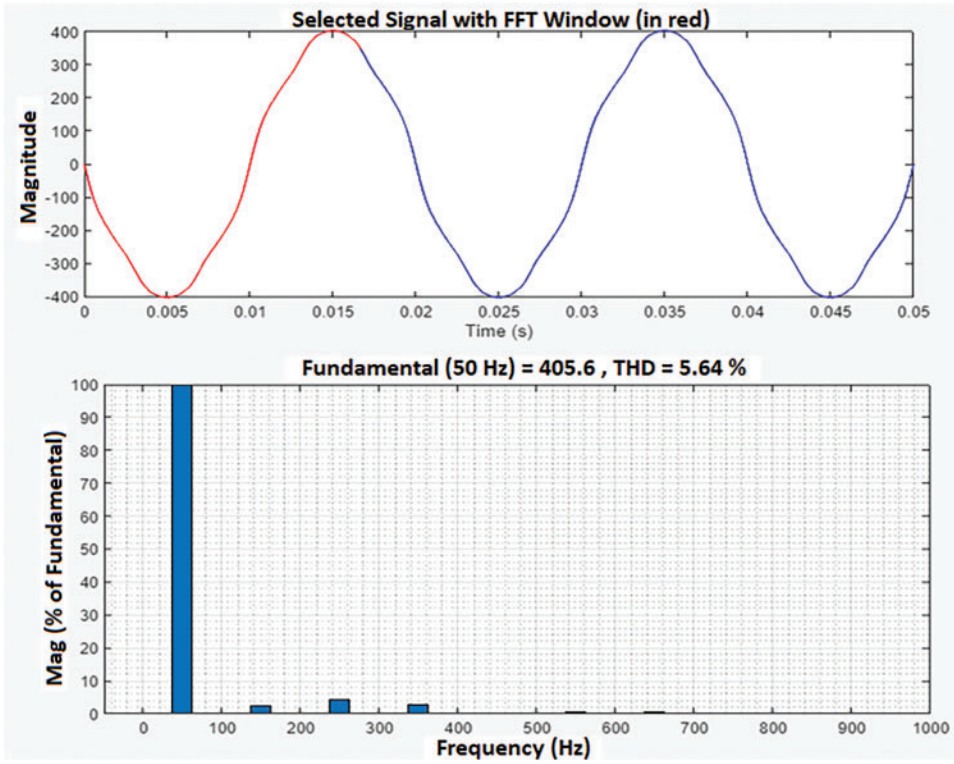

Figure A9: Fast fourier transformation graph at transformer 4

Appendix E

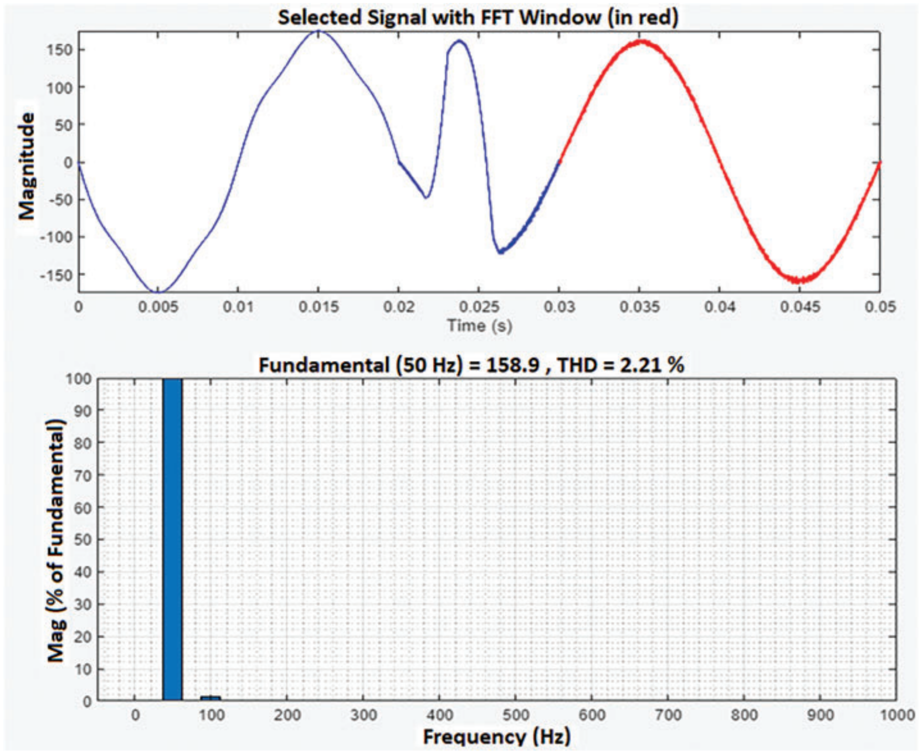

Figure A10: Fast fourier transform graph for transformer 2 with parallel active power filter activated

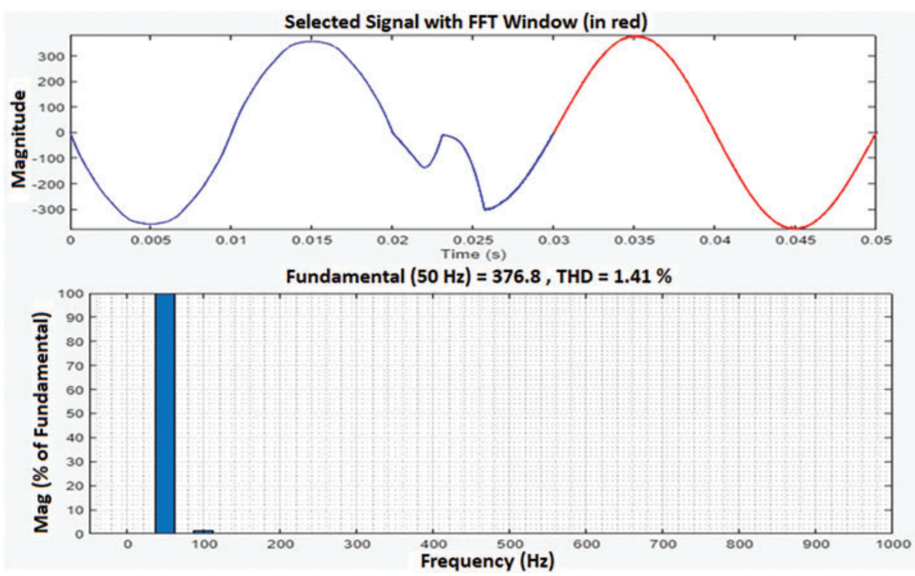

Figure A11: Fast fourier transform graph for transformer 3 with parallel active power filter activated

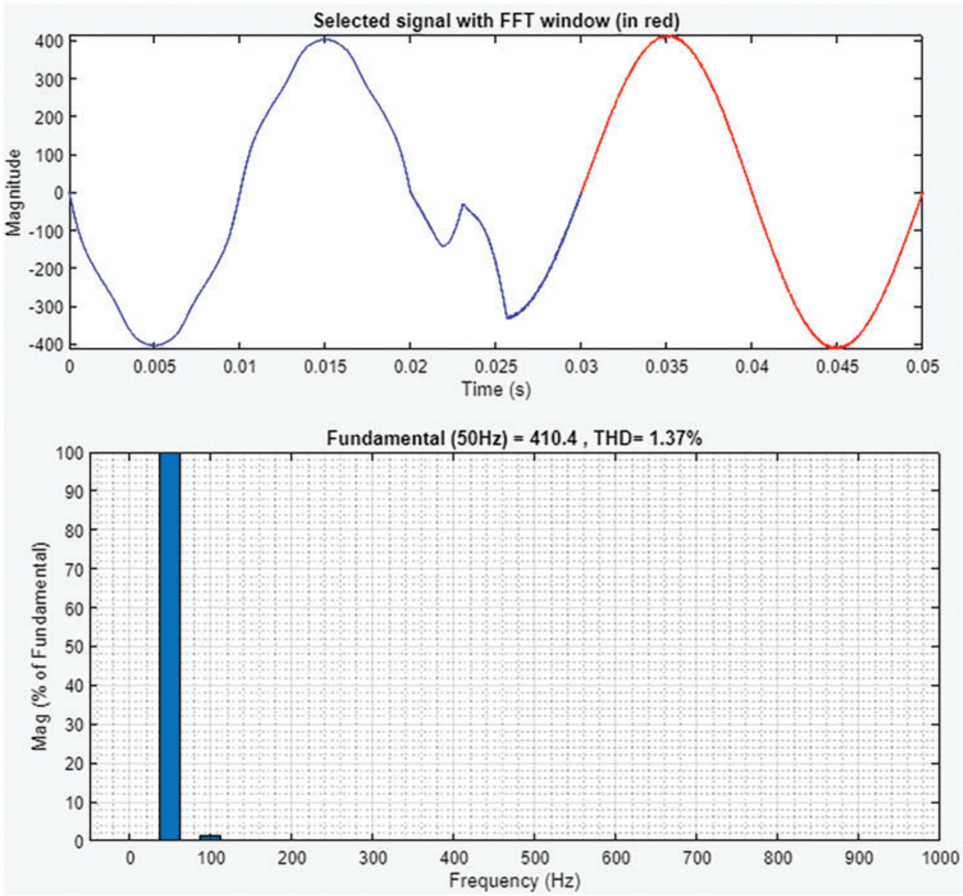

Figure A12: Fast fourier transform graph for transformer 4 with parallel active power filter activated